keV x-ray imaging of a fs laser plasma with a spherically curved crystal

K. Gäbel, R. Hannon, S. Grantham, M. Richardson, M. Kado, G. Shimkaveg

Laser Plasma Laboratory
CREOL, University of Central Florida
12424 Research Parkway, Suite 400
Orlando, Florida 32826

ABSTRACT

Images of a 130fs laser produced Ta-plasma were obtained with a spherically curved Mica crystal in four narrow spectral bands simultaneously. These are to our knowledge the first published x-ray images of a fs laser plasma. Also Mica was used for the first time as the imaging crystal. The resolved plasma size in the experiment (50μm·90μm) agrees with ray-tracing calculations and corresponds to the actual source size in our current setup. The four spectral bands of imaging are due to the strong Mica reflectivity in higher Bragg diffraction orders. All contributing bands have an energy higher than 1keV. Several laser shots were accumulated to achieve the required flux on the detector. Source spectroscopy was conducted to verify the source emission and the plasma density during the interaction with the 130fs laser pulse. Based on our experimental data the luminosity of crystal imaging is compared to a pinhole camera.

INTRODUCTION

X-ray imaging of laser produced plasmas for diagnostic purposes is routinely performed with pinhole cameras at most facilities. Inherently poor spectral resolution can be realized by an appropriate selection of thin foils and their λ-dependent transmission for x-rays.[1,2,3] Diagnostics relying on line intensity ratios require spectral resolution of the order of the line width, typically several mÅ, combined with spatial resolution of several microns.[4,5,6] The next generation of nuclear fusion devices like the National Igniter Facility will generate very dense plasmas, which require hard x-ray probes of several keV energy due to excessive absorption of lower energetic radiation.[7] Bragg reflectors are a natural choice in this energy region since efficient diffraction at the lattice of most crystals is within this range. Moreover an effective discrimination between probe radiation and background can be achieved since the crystal diffraction is intrinsically narrow band.

An additional interest in keV x-ray optics can be expected due to an increasing number of fs laser facilities at the TW level and numerous potential applications of hard x-ray sources of high brightness and short duration.[8,9,10,11,12]

Two-dimensionally curved crystal optics provide a unique combination of high spatial resolution, ≤10μm, and high spectral resolution between $10^2..10^4$. High spectral resolution is obtained since typical widths of reflection curves of plain and curved crystals are in the range of several 10 seconds of arc.[13]

0-8194-1882-X/95/$6.00

A spherically curved crystal in off axis geometry acts like a concave mirror for visible light with the exception that only radiation of the wavelength given by Bragg's law contributes to the image. The actual bandwidth of imaging depends on the chosen geometry and is determined by either the width of the reflection curve of the bent crystal or the angular aperture of the crystal in the dispersion plane. Magnification is obtained when the source to crystal distance is smaller than the radius of crystal curvature times $\sin\Theta_{Bragg}$ in accordance with imaging laws for off axis mirrors. The imaging bandwidth is coupled to the magnification and varies between $\Delta\lambda/\lambda=10^{-4}..10^{-2}$. The narrowest band is realized for unity magnification.[14]

CRYSTAL IMAGING OF A FS LASER PLASMA

Imaging of a Tantalum plasma was achieved with a spherically curved Mica crystal, radius of curvature 300mm, fabricated at the Laser Plasma Laboratory at CREOL. The fabrication of the spherically curved crystal optics follows the procedure described by Förster et al.[14] The thin Mica disc is brought in optical contact with a convex mirror blank to impose the blank's surface figure on the crystal. A concave counterpart of the blank is then epoxied to the second crystal surface. After the epoxy is cured the convex blank is removed and the crystal margins are covered with a Teflon mask. Figure 1 illustrates the process of crystal fabrication schematically.

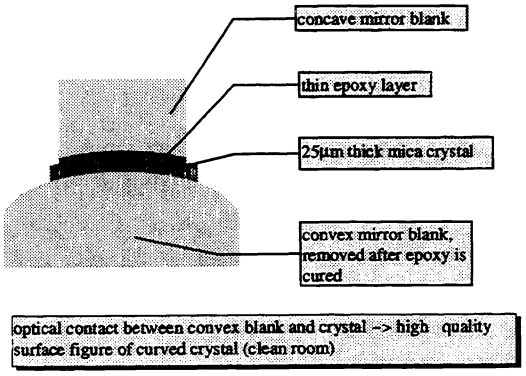

fig. 1 fabrication of spherically curved crystals

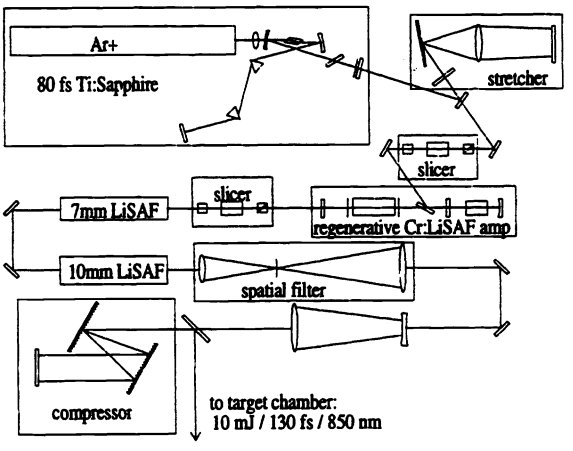

fig. 2 Ti:Sapphire/Cr:LiSAF CPA laser system

The plasma was created in the focus of our Ti:Sapphire/Cr:LiSAF CPA laser system.[15] Figure 2 shows the current laser setup. Pulses from an Argon-ion pumped 80fs Ti:Sapphire oscillator are stretched to 200ps duration. A birefringent tuner inside the Ti:Sapphire cavity forces the oscillator wavelength to 850nm, which is the peak of the Cr:LiSAF gain curve.[16] The first slicer selects a single pulse, which is injected in the Cr:LiSAF regenerative amplifier. A single pulse is selected by the second slicer from the train leaving the amplifier through the output coupler. This pulse is further amplified in single passes through 7mm diameter and 10mm diameter Cr:LiSAF power amplifiers. Before compression the pulse passes through a spatial filter. The current setup of the spatial filter in air prevents us from

double passing both amplifiers and reaching higher power of 0.5TW, measured without the spatial filter. After pulse compression 10mJ, 130fs pulses at 850nm are focused on target with a f/10 singlet lens yielding a peak intensity of $2 \cdot 10^{15} W/cm^2$. The intensity on target was calculated using the x-ray emitting area rather than the laser beam diffraction limit for reasons explained later on in the paper.
The crystal optic was arranged inside the target chamber to image the plasma source with unity magnification. The Bragg angle was set to 86° to minimize astigmatism, note that the Bragg angle is counted from the surface of the crystal. Figure 3 shows point spread functions (PSF) in the image plane for our geometry calculated for crystal aperture diameters of 8mm and 2mm respectively. The PSF's are calculated with a ray-tracing code, which assumes reflections at the crystal surface combined with a weighting procedure to account for narrow band effects due to x-ray diffraction at the crystal lattice.[14,17] In the case of the full crystal aperture the expected spatial resolution is rather moderate, 40μm, while an increase in resolution of a factor of 4 is achieved with 2mm aperture diameter. Note that the improved spatial resolution has to be traded-off by 4-times smaller aperture and hence 16-times lower luminosity.
To find the focus of the crystal optic the detector, Kodak DEF x-ray film, was moved around a predetermined focus position and the recorded spot was observed. 150 laser shots were necessary to achieve appropriate optical density on the film in the crystal focal plane when the full crystal aperture was used. Figure 4a shows a densitometer trace of the recorded x-ray image. The spot size is 50 μm·90μm. The image is not circular as expected but rather elongated. Figure 4b shows the image obtained with 2mm aperture diameter of the crystal at the optimized film position. 1800 shots were accumulated and slightly lower optical density was achieved. Although the image obtained with the smaller crystal aperture shows some indication of a double peak structure the general, elliptical shape is reproduced. Since the image size with both different apertures is essentially the same, the observed spot corresponds to the actual x-ray source size. Comparing the x-ray images to an atomic force microscope scan of the crater in a silicon target, used in the spectroscopy experiments, shows a close similarity of both pictures (figure 5). A careful examination of the laser beam reveals slightly different horizontal and vertical divergence after passing through the 7mm amplifier, thus the highest intensity on target can be obtained in an elliptical spot. We expect only a marginal increase of x-ray source size due to the accumulation of several shots, since the laser beam is passing through a pinhole in the spatial filter.

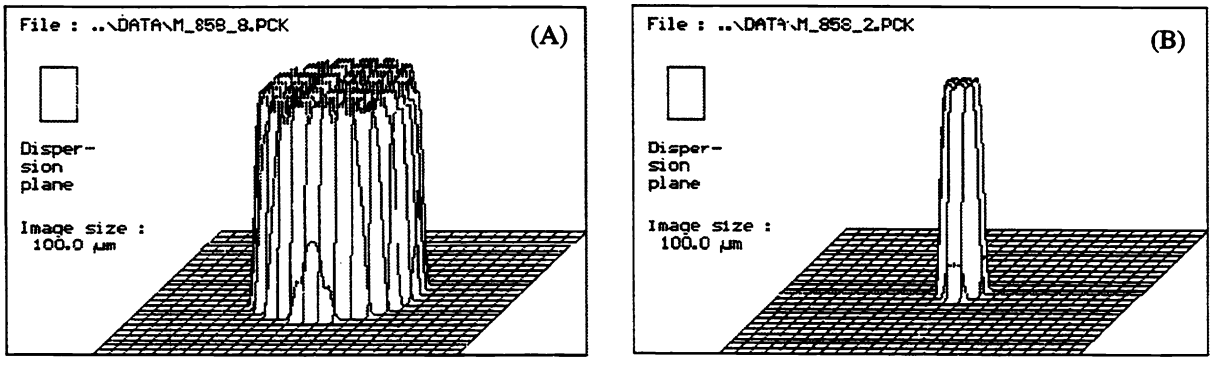

fig. 3 point spread functions for 2 different crystal apertures: 8mm diameter (A), 2mm diameter (B)

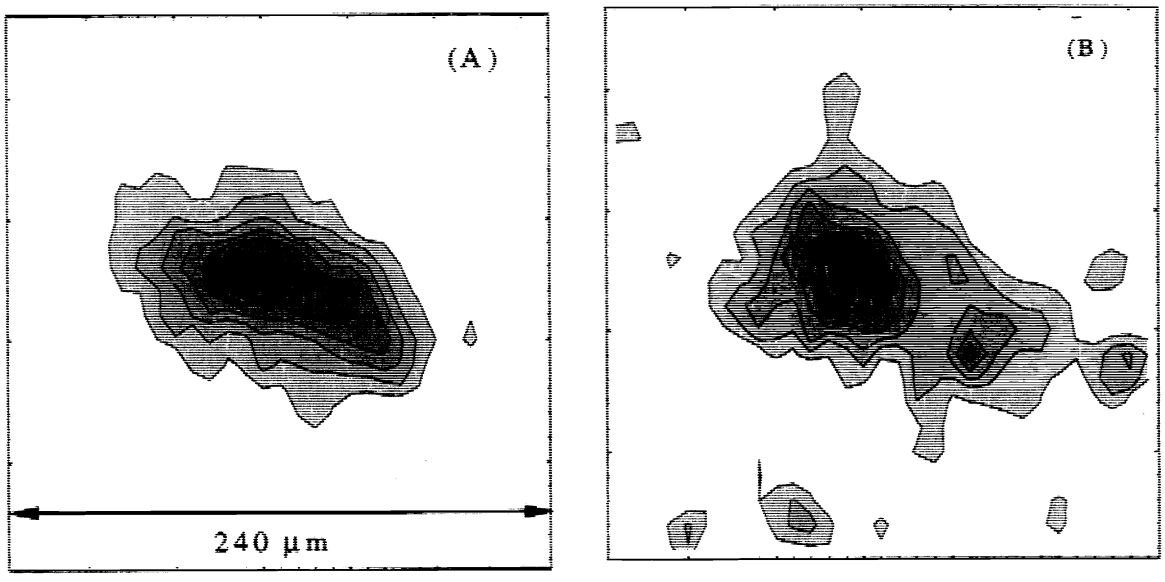

fig. 4 densitometer trace of x-ray image: 8mm aperture (A), 2mm aperture (B)

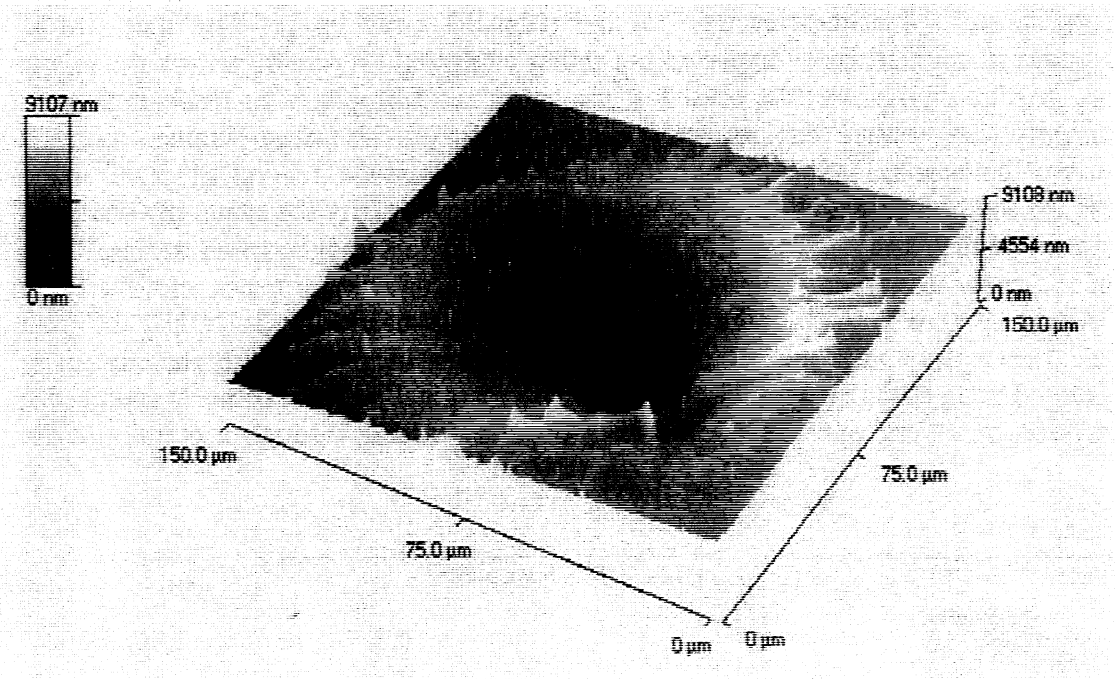

fig. 5 atomic force microscope scan of the crater in a Si-target

SOURCE SPECTROSCOPY AND LASER/PLASMA INTERACTION

Since higher reflection orders of Mica are strong, a careful examination of the source spectrum is necessary in order to determine the spectral components in the image.[18] A von Hamos spectrograph incorporating a cylindrically curved PET crystal was used to determine the keV-spectrum of low Z

(Silicon) and high Z (Tantalum) targets.[19] The particular spectrograph was chosen because of it's high luminosity due to the focusing of x-rays perpendicular to the dispersion plane of the cylindrically curved crystal. Moreover the PET composition of only low Z elements prevents x-ray fluorescence in the crystal itself which can cause a keV-background on the detector. The measured Ta-spectrum can be approximated with blackbody radiation at 500eV, and the emission peak at 2keV. Figure 6 shows the combined effects of Mica reflectivity, source spectrum, Be-filter transmission, and Kodak DEF sensitivity on the spectral bands contributing to the image. Energy below 1keV is effectively cut-off since source emission, Be-transmission and film response drop rapidly with decreasing energy. With exception of a small spectral contribution at 1keV the image is formed essentially in three narrow bands around 2keV. Note that the width of these spectral bands is highly exaggerated in figure 6, in our experiments $\Delta\lambda/\lambda$ was $2{\cdot}10^{-3}$ for the full crystal aperture and $5{\cdot}10^{-4}$ for the 2mm crystal aperture.

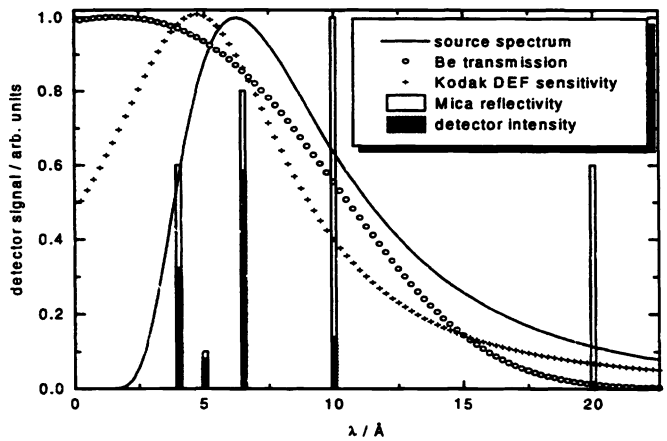

fig. 6 spectral components in x-ray image, determined by Ta:spectrum, crystal reflectivity, filter transmission, and detector response

K-shell line spectra obtained with a Silicon target can be used to determine the parameters of the laser/plasma interaction. Figure 7 shows a densitometer scan of the Si-spectrum between the He_α and the K_α lines. The presence of the intercombination line indicates that the main, fs-pulse interacts with a plasma well below solid density, while the dominating K_α line is caused by hot electrons slammed into a weakly ionized, cold plasma which is characteristic for fs interaction.[20,21,22] The lines between the He_α satellites and K_α represent K-shell resonance transitions in species of $Si^{5+}..Si^{11+}$ ionization states. The laser/plasma interaction below solid density is caused by a ns ASE background strong enough to create a pre-plasma in which the fs-pulse is coupled. Even in the presence of an ASE caused pre-plasma the x-ray source size is expected to correspond to the focus size of the laser beam because the excitation of keV x-rays originates from the fs laser pulse. Hence it will terminate in a time short compared to the ns time scale of plasma expansion.[23] A schematic illustration of the single slicer leakage (contrast $\leq$1000) and the effect on the laser/plasma interaction is presented in figure 8, note that the contrast is exaggerated in the figure. Pre-cursor pulses, which leak through the slicer are strong enough to create plasmas on target. Hence the main pulse, which arrives with an integer·10ns delay, passes through a very diluted plasma without any important interaction. The major effect is excessive debris, since the main pulse hits a crater produced by the pre-cursors.

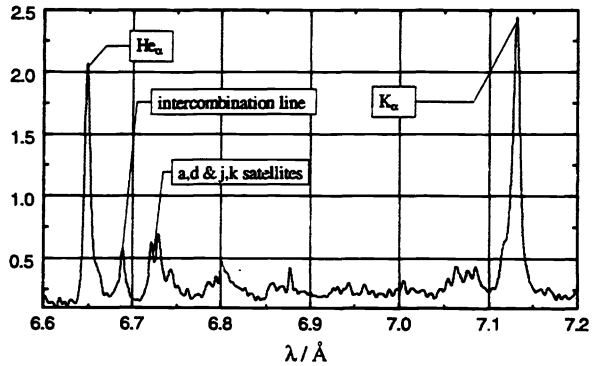

fig. 7 densitometer scan of Si-spectrum

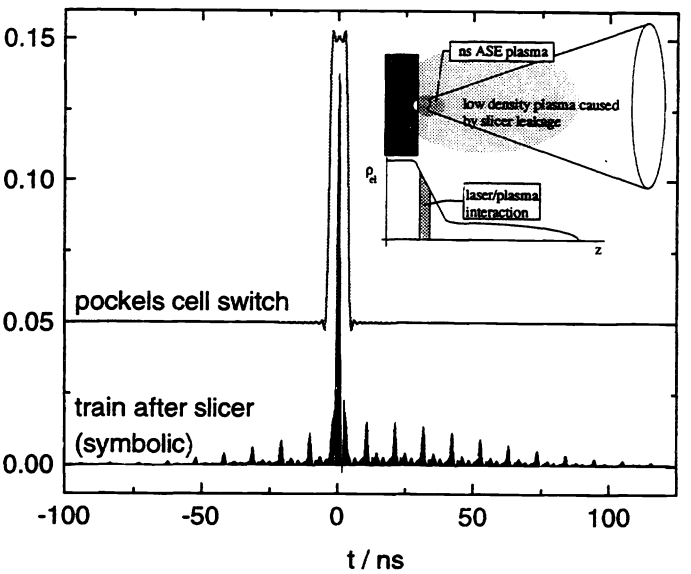

fig. 8 slicer leakage and laser/plasma interaction (schematic)

CRYSTAL OPTICS LUMINOSITY

Finally we performed an experimental luminosity comparison of the crystal optics and a pinhole camera. A simple estimate for the intensity ratio at the detector element dxdy in case of the crystal optics ($I_{crystal}$) and the pinhole camera (I_{phc}) is given by the following equation:

$$\left.\frac{I_{crystal}}{I_{phc}}\right|_{dxdy} = \left(\frac{d_{crystal.aperture} \cdot l_{source-film.phc}}{d_{psf} \cdot l_{source-crystal}}\right)^2 \cdot R_{peak}$$

l denotes distances from the plasma to the spherically curved crystal and from the plasma to the film respectively, $d_{crystal.aperture}$ is the diameter of the crystal aperture, d_{PSF} is the diameter of the point spread function calculated via ray-tracing, and R_{peak} is the Mica peak reflectivity for monochromatic radiation of a particular wavelength. R_{peak} is between 10%..50% under our experimental conditions, with 4 diffraction orders contributing to the image. Hence a gain of ~5000 can be expected with crystal optics, if both devices use the same bandwidth of imaging. It was found in the experiments, that similar optical density on the detector is realized for a 1:2 ratio of shots with the pinhole camera and the crystal optics respectively. Thus the spectral resolution of the crystal optics is traded-off by a slight decrease of luminosity for a broad band source. Increased luminosity can be expected for a source which emits dominantly in a few spectral lines, if one of these lines is used for crystal imaging.

CONCLUSIONS

In conclusion we have demonstrated for the first time to our knowledge x-ray imaging of a sub-100μm size fs laser produced plasma using a 2-dimensionally curved crystal.
Although spherically curved Mica crystals were used for spectroscopy before, no imaging with this particular material was achieved.[24] Mica offers the advantage of extending the wavelength range for monochromatic crystal imaging beyond 8.5Å, which is the current limit with Quartz.
Plasma images of the same size were obtained for two different crystal apertures which is consistent with an image size determined bye the x-ray source rather than crystal optics aberrations.
The imaged source shape corresponds to the crater shape observed with an atomic force microscope.
Analysis of the source spectrum leads to identification of the spectral components in the image which are primarily at 2keV. Spectral resolution between 500 and 2000 was achieved in four well separated bands, which can be discriminated by filter techniques. X-ray spectroscopic results of a low Z target indicate an ASE-produced pre-plasma, which prevents us from generating harder x-rays by coupling into a steep density gradient.[25] Experimental data comparing pinhole and crystal imaging demonstrate that the high spectral resolution of the crystal optics is only accompanied by a factor of 2 loss in luminosity for our broad band source.
The experimental results illustrate the feasibility of a table top CPA laser system for the characterization of crystal optics at their design wavelength, since x-rays should be obtained in a quasi point source and an intensity of $10^{17}W/cm^2$ is generated on target with a medium size facility allowing x-ray production at any energy up to at least 10keV.
To increase the spatial resolution we intend to fabricate toroidally curved crystals, which are free of astigmatism at the design wavelength. Crystals will be selected to image plasmas with 6..10keV x-rays. Frequency up-conversion of the laser is planned to reduce the ASE background and thus to produce the required steep density gradient for hard x-ray generation. Correction of the laser beam divergence and incorporating a parabolic off-axis laser mirror is intended to achieve a diffraction limited spot and higher intensity on target. A vacuum spatial filter will allow us to double pass amplifiers and to create enough x-ray flux for single shot imaging.

ACKNOWLEDGEMENT

We like to thank Dr. Ch. Brown and K. Abbott of NRL, Washington DC, for the densitometer traces of our x-ray films. We acknowledge the support of the Max Planck Gruppe 'Röntgenoptik' in Jena which provided us with the von Hamos spectrograph. We are grateful to S&J Trading Inc. for supporting us with the Mica material. Also we like to thank Dr. G. Stegeman from CREOL for the use of his clean room and Dr. O. L. Landen from LLNL for providing us with references on NOVA imaging techniques.

This work was funded by Lawrence Livermore National Laboratories under contract #80942, and by the State of Florida. M. Kado is supported by the Japanese Society for the Promotion of Science.

REFERENCES

[1] O. L. Landen, Rev. Sci. Instrum. 63, 5075 (1992)
[2] H. Shiraga, M. Heya, A. Fujishima, O. Maegawa, K. Shimada, Y. Kato, T. Yamanaka, and S. Nakai Rev. Sci. Instrum. 66, 722 (1995)
[3] D. T. Attwood, B. W. Weinstein, and R. F. Wuerker, Appl. Opt. 16, 1253 (1977)
[4] D. Duston and J. Davis, Phys. Rev. A 21, 1664 (1980)
[5] R. S. Marjoribanks, M. C. Richardson, P. A. Jaanimagi, and R. Epstein, Phys. Rev. A 46, R1747 (1992)
[6] A. V. Vinogradov, I. Yu. Skobelev, and E. A. Yukov, Sov. J. Quant. Electron. 5, 630 (1975)
[7] S. G. Glendinning, 'Laser plasma diagnostics of dense plasmas', SPIE Proceedings Vol. 2523, 2523-03 (1995)
[8] T. Ditmire and M. D. Perry 'Amplification of fs pulses to 1J in Cr:LiSAF', Technical Digest CLEO '95, CFD7 (1995)
[9] A. Sullivan, H. Hamster, H. C. Kapteyn, S. Gordon, W. White, N. Nathel, R. J. Blair, and R. W. Falcone, Opt. Lett. 16, 1406 (1991)
[10] W. E. White, D. F. Price, J. D. Bonlie, and R. E. Stewart 'Production of 10TW, 100fs pulses using Nd:glass pumped Ti:Sapphire', Post Deadline Digest Cleo '95, CPD45 (1995)
[11] C. P. J. Barty 'Time gated medical imaging with ultrafast laser plasma x-rays', SPIE Proceedings Vol. 2523, 2523-32 (1995)
[12] C. L. Gordon III, G. Y. Yin, B. E. Lemoff, P. M. Bell, and C. P. J. Barty, Opt. Lett., 20, 1056 (1995)
[13] I. Uschmann, E. Förster, K. Gäbel, G. Hölzer, M. Ensslen, J. Appl. Cryst. 26, 405 (1993)
[14] E. Förster, K. Gäbel, and I. Uschmann, Laser & Particle Beams 9, 135 (1991)
[15] P. Beaud, M. Richardson, E. J. Miesak, and B. H. T. Chai, Opt. Lett. 18, 1550 (1993)
[16] S. A. Payne, L. L. Chase, L. K. Smith, W. L. Kway, H. W. Newkirk, J. Appl. Phys. 66, 1051 (1989)
[17] K. Gäbel, PhD thesis, Friedrich Schiller Universität Jena (1991)
[18] E. M. Gullikson, 'Low energy x-ray and electron physics and technology for high temperature plasma diagnostics', Unsolicited Proposal for the Continuation of DOE Research Contract No. SAN # CID #9501, Task I, Center for X-Ray Optics, Lawrence Berkley Laboratory, June 1987
[19] P. Audebert, J. P. Geindre, J. C. Gauthier, A. Mysyrowicz, J. P. Chambarret, and A. Antonetti, Europhys. Lett. 19, 189 (1992)
[20] J. C. Kieffer and M. Chaker, J. X-Ray Sci. Technol. 4, 312 (1994)
[21] S. P. Gordon, T. Donnelly, A. Sullivan, H. Hamster, and R. W. Falcone, Opt. Lett.19, 484 (1994)
[22] R. Benattar, J. P. Geindre, P. Audebert, J. C. Gauthier, A. Mysyrowicz, J. P. Chambarret, and A. Antonetti, Opt. Comm. 88, 376 (1992)
[23] J. C. Kieffer and M. Chaker, J. X-Ray Sci. Technol. 4, 312 (1994)
[24] B. A. Bryunetkin, A. Ya. Faenov, S. A. Pikuz, and I. Yu. Skobelev, Laser & Particle Beams 10, 849 (1992)
[25] J. D. Kmetec, IEEE J. Quant. Electron. 28, 2382 (1992)